

Breaking Modality Gap in RGBT Tracking: Coupled Knowledge Distillation

Andong Lu*, Jiacong Zhao[†], Chenglong Li[†], Yun Xiao[†] and Bin Luo*

*School of Computer Science and Technology, Anhui University

[†]School of Artificial Intelligence, Anhui University

adlu_ah@foxmail.com

Abstract—Modality gap between RGB and thermal infrared (TIR) images is a crucial issue but often overlooked in existing RGBT tracking methods. It can be observed that modality gap mainly lies in the image style difference. In this work, we propose a novel Coupled Knowledge Distillation framework called CKD, which pursues common styles of different modalities to break modality gap, for high performance RGBT tracking. In particular, we introduce two student networks and employ the style distillation loss to make their style features consistent as much as possible. Through alleviating the style difference of two student networks, we can break modality gap of different modalities well. However, the distillation of style features might harm to the content representations of two modalities in student networks. To handle this issue, we take original RGB and TIR networks as the teachers, and distill their content knowledge into two student networks respectively by the style-content orthogonal feature decoupling scheme. We couple the above two distillation processes in an online optimization framework to form new feature representations of RGB and thermal modalities without modality gap. In addition, we design a masked modeling strategy and a multi-modal candidate token elimination strategy into CKD to improve tracking robustness and efficiency respectively. Extensive experiments on five standard RGBT tracking datasets validate the effectiveness of the proposed method against state-of-the-art methods while achieving the fastest tracking speed of 96.4 FPS. Code available at <https://github.com/Multi-Modality-Tracking/CKD>.

I. INTRODUCTION

In recent years, the field of RGBT tracking attracts great attention due to its wide range of applications in surveillance, object recognition and other fields [1]–[10]. RGBT tracking aims to take advantage of the complementary advantages of RGB and thermal modalities to achieve robust object tracking. However, visible spectrum and thermal infrared data are collected by cameras in different imaging bands, reflecting different properties of the target object. As a result, they differ significantly in appearance style, which inevitably leads to the issue of modality gap.

Current research on RGBT tracking focuses on three categories, including multi-modal fusion design, multi-modal representation learning, and prompt learning. The first category of studies [1], [12] are usually devoted to designing a reliable late fusion module for the collaboration between RGB and thermal infrared (TIR) modality features. For instance, Liu *et al.* [12] proposes a quality-aware fusion module that carefully designs two independently weighted prediction branches to guide the fusion of multi-modal features. The second category

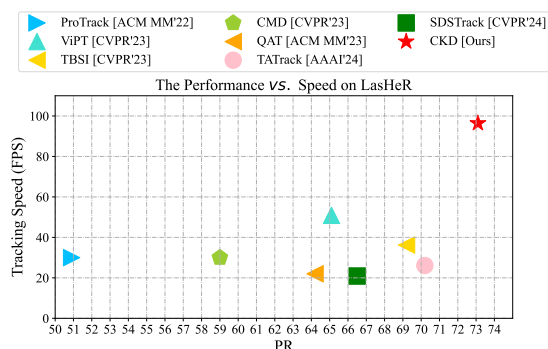


Fig. 1. Comparison of performance and speed for state-of-the-art tracking methods on LasHeR [11]. We visualize the Precision Rate (PR) to the Frames Per Second (FPS). CKD is able to rank the 1st in PR while running at 96.4 FPS.

of research [3], [5], [13], [14] focus on integrating multi-layer feature interaction modules into backbone network, thus can leverage modality complementary information to enhance the representation of each modality. For example, Hui *et al.* [5] introduce a Transformer-based multi-layer feature interaction module, which effectively enhances the exchange of information between modalities. The third category of methods [6], [15], [16] explore the concept of prompt learning in multi-modal feature interaction. For example, Cao *et al.* [6] design a bi-directional adapter for mutual prompting of modality information. However, existing studies have long overlooked the influence of modality gap, thus limiting the performance and efficiency of current RGBT tracker.

To address this challenge, we propose a novel Coupled Knowledge Distillation framework (CKD), which pursues common styles of different modalities to break modality gap, for high performance RGBT tracking. Figure 1 presents the advantages of CKD compared to existing state-of-the-art methods in two different dimensional metrics, which suggest a powerful potential in breaking modality gap. Specifically, we analyse the impact of modality style on the modality gap in Figure 2, which can be seen that the modality gap is significantly reduced after removing the modality style. Therefore, the modality style plays an important factor in breaking modality gap. However, the structure of the modal feature distribution is also affected, which may harm the modal content representation.

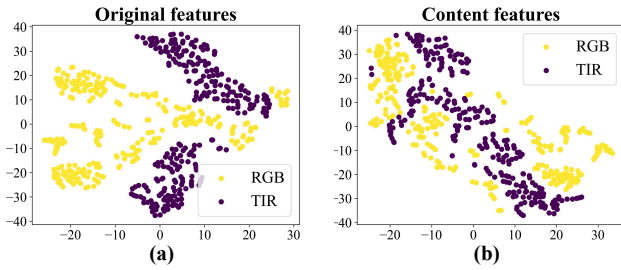


Fig. 2. Illustration of the influence of modality style on modality gap. Here, (a) denotes the feature distribution of the two modalities, and (b) denotes the feature distribution of the two modalities after removing the style information using instance normalization.

To this end, we introduce two student networks and design a style distillation scheme between the style features of the two students to make their style features as consistent as possible, aiming to eliminate the modality gap. Here, we utilize the feature mean and standard deviation to represent the style features of a modality, which has been proven to be effective in many studies [17], [18]. However, style feature distillation may harm modality content representations of both student branches. We further introduce the original RGB and TIR networks as teachers, and design a content distillation scheme to pursue the consistency between the content features of the teacher branch and the corresponding student branch. To alleviate the constraints on student style features, we employ a style-content orthogonal feature decoupling strategy that obtains content features by performing instance normalization on the original features. Consequently, we couple the above two distillation processes in an online optimization framework to pursue the common style of the two modalities while avoiding the damage to the modality content representation.

In addition, we design a masked modeling strategy to further enhance the robustness of modality features in challenging scenarios. It involves the random mask to create data pairs of content-degraded and non-degraded of one modality, and then feed into the teacher and student branches. We can employ content distillation loss in CKD to effectively learn representations for content reconstruction. We also design a simple and effective multi-modal candidate token elimination strategy, which collaboratively considers the information of the two modalities to jointly decide the candidate elimination tokens in the search region. By drop these tokens during the inference phase, we can achieve a balance between tracking performance and tracking efficiency.

In summary, our major contributions are as follows.

- We propose a novel coupled knowledge distillation framework CKD to handle the modality gap issue by eliminating the style difference between RGB and thermal images for high performance RGBT tracking. To the best of our knowledge, this research is the first effort to break the modality gap in RGBT tracking.
- We design a style-content coupled distillation scheme based on style-content orthogonal feature decoupling,

which effectively eliminates modality gap without harming the modality content representation.

- We present a masked modeling scheme that is seamlessly integrated into CKD, which effectively enhances the learning of modality content representation. In addition, a multi-modal candidate token elimination strategy is designed, which further improves the tracking efficiency.
- The proposed method achieves an impressive tracking speed of 96.4 FPS while achieving state-of-the-art results on four mainstream public datasets. Compared with the existing methods, the PR/SR scores on RGBT210, RGBT234, LasHeR and VTUAV datasets are increased by 1.6%/2.7%, 1.6%/3.0%, 3.0%/2.0% and 10.1%/11.1%, respectively, and the speed is increased by 60.2 FPS.

II. RELATED WORK

A. RGBT Tracking

RGBT tracking, as a rapidly growing research field, has witnessed a significant surge in the development of innovative algorithms. Existing studies can be broadly classified into three categories, including multi-modal fusion design, multi-modal representation learning and prompt learning. The first category [12], [19]–[21] is dedicated to designing diverse fusion strategies that combine the features of two modalities. Liu *et al.* [12] employ feature weighted fusion architectures based on the importance or quality of each modality. Tang *et al.* [21] apply modal weighting fusion strategy to three different levels of pixel, feature and decision. However, the optimal level of fusion varies in different scenarios. The second category [1], [3], [5], [14], [22], [23] is devoted to the improvement of modal representation by feature decoupling or feature interaction. For instance, Li *et al.* [1], [22] design a multi-adapter framework to simultaneously extract modality-shared and modality-specific features. Similarly, Zhang *et al.* [23] design a multi-branch challenge framework to model modality representation under different challenge scenarios. Lu *et al.* [3] design multi-layer feature interaction modules to enhance the modality representation. The third category [6], [15], [16], [24], [25] focuses on modal information interaction in a prompting manner, and is also a recent hot research topic. For example, Yang *et al.* [16] and Zhu *et al.* [15] introduce the concept of prompt learning at the pixel level and the feature level of RGBT tracking, respectively, for efficient multi-modal tracking. However, these methods ignore the impact of modality gap, which limits the RGBT tracking performance.

B. Knowledge Distillation

Knowledge distillation [26] aims to transfer the knowledge from a pre-trained large-scale teacher model to a small-scale student model. According to the type of knowledge transferred, the current research is mainly divided into three categories. Probability-based methods [26], [27] leverage the teacher model’s predicted probabilities, guiding the student model to emulate the teacher’s log-class distribution through minimizing KL divergence. Conversely, Feature-based methods [28]–[30]

harness the mid-layer output feature map of the network for supervising the training of the student model. Relation-based methods [31], [32] emphasize inter-sample relationships over single instances. While simple to implement, it requires complex teacher modeling and significant training time. To address these issues, some studies [33], [34] utilize a mutual learning strategy for knowledge transfer. In addition, cross-modality knowledge distillation aims to transfer knowledge between different modalities. Some studies [35], [36] use dominant modality to guide weaker ones, while others [37], [38] investigate inter-modal complementarity. In contrast to existing methods, the coupled knowledge distillation method proposed in this paper distills coupled modality content and modality style knowledge from different modalities, thus facilitating modality style transfer for modality content preservation achievable by student models.

III. METHODOLOGY

In this section, we first introduce the overall architecture of Coupled Knowledge Distillation (CKD) and then describe the coupled knowledge distillation approach. Subsequently, mask modeling and multi-modal candidate token elimination are introduced. Finally, the training process and implementation details are given.

A. Framework Overview

We provide a detailed description of CKD framework, and its overall structure is shown in Figure 3. During the training phase, our CKD framework comprises four branches (including a RGB teacher branch, a TIR teacher branch, a RGB student branch, and a TIR student branch) as well as three tracking heads (including a multi-modal tracking head and two single-modal tracking heads). In the testing phase, CKD consists of two student branches and one multi-modal tracking head. In specific, for the given RGB and TIR modal frames, the search and template frames are first partitioned into patches with the size of $p \times p$ using four independent learnable patch embedding layers, and flattened to obtain four search token sequences ($S_{rgb}^t, S_{tir}^t, S_{rgb}^s, S_{tir}^s$), and four template token sequences ($T_{rgb}^t, T_{tir}^t, T_{rgb}^s, T_{tir}^s$). Following [39], we also add learnable position embeddings to the above tokens to provide positional prior information. Note that we add random mask to the search frame token sequences (S_{rgb}^s, S_{tir}^s) in the two student branches during training.

Then, we concatenate search and template frame token sequences for the four groups, denoted as $I_{rgb}^t = [S_{rgb}^t, T_{rgb}^t]$, $I_{tir}^t = [S_{tir}^t, T_{tir}^t]$, $I_{rgb}^s = [S_{rgb}^s, T_{rgb}^s]$, and $I_{tir}^s = [S_{tir}^s, T_{tir}^s]$. We feed I_{rgb}^t and I_{tir}^t into the RGB and TIR teacher branches, respectively, while I_{rgb}^s and I_{tir}^s into the RGB and TIR student branches, respectively. These branches share an identical structure, consisting of standard Transformer blocks [40], but they have independent parameters. Finally, we concatenate the last layer features of the RGB and TIR student branches in the channel dimension and input them into the tracking head [39] for object localization and regression. The last layer features

of the RGB and TIR teacher branches are separately fed into two independent tracking head [39] networks for task learning.

B. Coupled Knowledge Distillation

The proposed CKD is the first effort in the field of RGBT tracking to address modality gap. In particular, CKD employs a style distillation to make the style features of the two modalities as consistent as possible, thus breaking modality gap. It also introduces a content distillation to ensure that the modality content representation is stable. Next, we describe two distillation methods, namely style distillation and content distillation, in detail.

1) *Style Distillation*: Style distillation aims at mutual distillation between the style features of the two student branches, thus pursuing a common style for both modalities to break modality gap. Feature style usually involves the statistical attributes of features, and existing studies [18] usually use the mean and standard deviation of features to represent feature style. Therefore, these two statistical attributes are adopted as feature styles in this study. Specifically, given the intermediate feature $f_{tir}^l \in \mathcal{R}^{B \times N \times D}$ from TIR student branch and $f_{rgb}^l \in \mathcal{R}^{B \times N \times D}$ from RGB student branch, where l denotes the feature from the l -th layer, B , N , and D represent the batch size, number of tokens, and channel dimension of tokens, respectively. For brevity, the B dimension is omitted below. The process of calculating the mean and standard deviation vectors of the two student branch features is as follows:

$$\mu_{rgb}^{s(l)} = \frac{1}{N} \sum_{n=1}^N f_{rgb}^{l(n)}, \quad \sigma_{rgb}^{s(l)} = \sqrt{\frac{1}{N} \sum_{n=1}^N (f_{rgb}^{l(n)} - \mu_{rgb}^{s(l)})^2}, \quad (1)$$

$$\mu_{tir}^{s(l)} = \frac{1}{N} \sum_{n=1}^N f_{tir}^{l(n)}, \quad \sigma_{tir}^{s(l)} = \sqrt{\frac{1}{N} \sum_{n=1}^N (f_{tir}^{l(n)} - \mu_{tir}^{s(l)})^2}. \quad (2)$$

where $\mu_{rgb}^{s(l)}$ and $\sigma_{rgb}^{s(l)}$ represent the mean and standard deviation vectors of RGB student features, respectively, while $\mu_{tir}^{s(l)}$ and $\sigma_{tir}^{s(l)}$ indicate the corresponding vectors for TIR student features. Then, we can compute the style distillation loss, denoted as \mathcal{L}_{SD} , by quantifying the mean squared error between the style features across all layers of the two student branches.

$$\mathcal{L}_{SD} = \frac{1}{L} \sum_{l=1}^L ((\mu_{tir}^{s(l)} - \mu_{rgb}^{s(l)})^2 + (\sigma_{tir}^{s(l)} - \sigma_{rgb}^{s(l)})^2). \quad (3)$$

By minimizing this style distillation loss during training, we can achieve style consistency across different modality features.

2) *Content Distillation*: Although RGB and TIR features of two student branches can eliminate modal gaps through style distillation, this process may harm the modal feature content representation. To alleviate this issue, we perform content distillation between teacher and student branches with the same modality input. To avoid imposing constraints on the style features in student branch, we adopt the classical instance

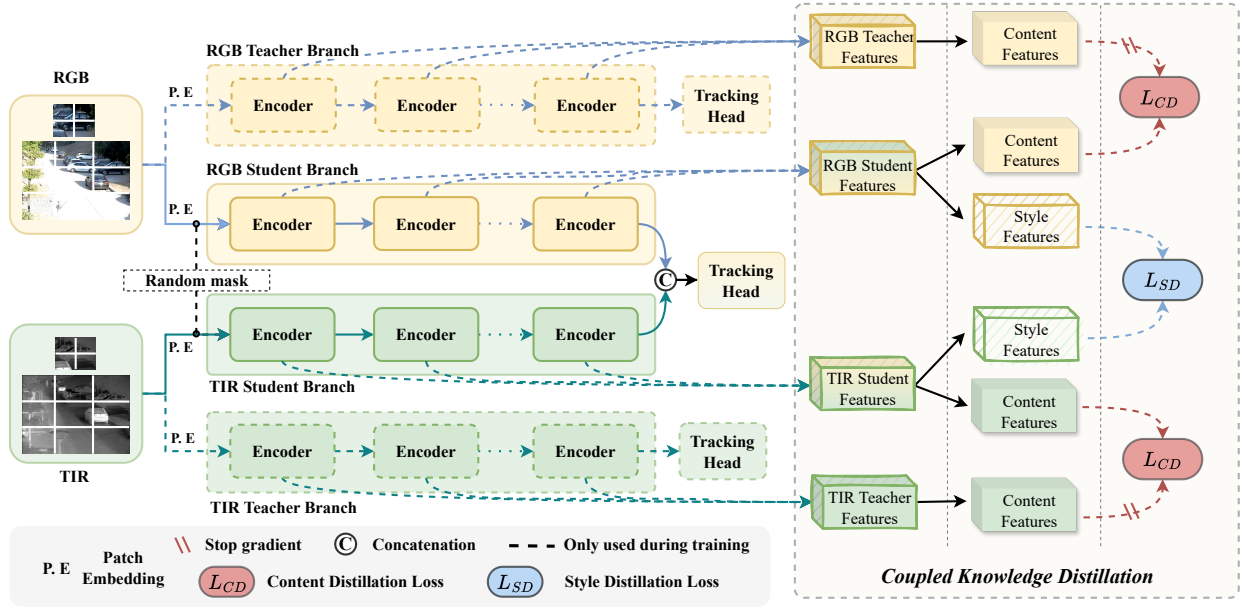


Fig. 3. Overall architecture of the proposed CKD. It mainly consists of a four-branch network, three tracking heads, and a coupled distillation framework. The four-branch network extracts visual features from the input video frames and performs style distillation and content distillation in the coupled distillation framework.

normalization operation to normalize teacher and student features, thus obtaining content features that are orthogonal to the style features. We can then calculate the similarity between the content features of the two groups of teachers and students for content distillation.

In particular, we take the TIR modality as an example and can describe above process as follows. Firstly, we perform feature instance normalization along the channel dimension as follows:

$$\hat{F}_{tir}^l = \frac{F_{tir_d}^l - \mu_{tir_d}^t}{\sigma_{tir_d}^t}, \hat{f}_{tir}^l = \frac{f_{tir_d}^l - \mu_{tir_d}^s}{\sigma_{tir_d}^s}. \quad (4)$$

where F_{tir}^l denotes the intermediate feature from TIR teacher branch, d represents the d -th channel dimension of each token. \hat{F}_{tir}^l represents the l -th layer normalized feature (i.e., content feature) of TIR teacher branch, and \hat{f}_{tir}^l denotes the l -th layer content feature of student branch. μ_{tir}^t , σ_{tir}^t , μ_{tir}^s , and σ_{tir}^s correspond to the mean and standard deviation, respectively. Subsequently, we calculate the TIR feature content distillation loss, denoted as \mathcal{L}_{CD}^{tir} , by measuring the mean squared error (MSE) between the content features across all layers of teacher and student branches:

$$\mathcal{L}_{CD}^{tir} = \frac{1}{L} \sum_{l=1}^L (\hat{F}_{tir}^l - \hat{f}_{tir}^l)^2. \quad (5)$$

Minimizing this loss during training ensures consistency between the content features of TIR student branch and those of TIR teacher branch. Similarly, this approach is applied in RGB student branching learning by incorporating a constraint from RGB teacher branch to maintain stability in content features.

Therefore, the total content distillation loss can be defined as follows:

$$\mathcal{L}_{CD} = \mathcal{L}_{CD}^{tir} + \mathcal{L}_{CD}^{rgb}. \quad (6)$$

where \mathcal{L}_{CD}^{rgb} denotes the RGB feature content distillation loss.

In summary, coupled knowledge distillation is a combination of style distillation and content distillation that can break the modality gap in RGBT tracking. Thus, by incorporating CKD into our task, we can train two student branches that extract style-consistent features from different modalities while preserving their individual semantic content features.

C. Masked Modeling

Inspired by recent success and scalability of pretraining with masked reconstruction in different domains [41], [42], we design a novel masked modeling in the proposed framework to enhance modality content representation in challenging scenarios. Since there is natural feature content supervision between teacher and student branches of the same modality input in CKD, we can implement mask modeling without introducing any additional loss and design, simply by applying random mask to the input of student branches.

In particular, we randomly mask some of the input tokens of a student branch with $m \in \{0, 1\}^N$, where N is the number of tokens. Hence the masked tokens are represented as $\{I_{rgb}^s | m_i = 1\}$ and $\{I_{tir}^s | m_i = 1\}$ while the remain tokens are denoted as $\{I_{rgb}^s | m_i = 0\}$ and $\{I_{tir}^s | m_i = 0\}$. Subsequently, we feed these tokens into the corresponding student branches, respectively. It is noteworthy that the input tokens for corresponding teacher branch remain unchanged. Consequently, we can utilize the token features from two teacher branches to guide the feature learning of the masked

tokens in two student branches. In fact, the aforementioned process can be realized by minimizing the content distillation loss, which seeks feature content consistency between the masked student tokens and the teacher tokens. Therefore, the masked modeling can be seamlessly integrated into CKD. In addition, we set the mask ratio as 25% empirically.

D. Multi-modal Token Elimination

The effectiveness of using candidate elimination strategies to provide inference efficiency has been demonstrated in [39]. Specifically, existing RGB trackers determine which tokens to eliminate by leveraging the attention weights established by the tokens in target and search regions. However, this strategy ignores that the elimination results are unreliable when the input data are of poor quality. To address this issue, we propose a multi-modal candidate token elimination strategy, which aims to improve elimination quality in challenging scenarios by combining attention weights of two modalities through cooperative decision making. Given the query vector q_r^{zi} from RGB template queries and the query vector q_t^{zi} from TIR template queries, a scalar h_i is assigned to each token in the search region, calculated as follows:

$$h = \max(\text{softmax}(q_r^{zi} k_r^x), \text{softmax}(q_t^{zi} k_t^x)) \quad (7)$$

where k_r^x and k_t^x represent the key vectors of tokens in the search region. We use h to sort the tokens in the search region and keep the top-k tokens. Therefore, the proposed method not only enhances the robustness of token elimination in challenging scenarios, but also improves the inference speed of the model.

E. Final Loss

In CKD, we can define the final loss function as a combination of content distillation, style distillation, and task losses, as follows:

$$\mathcal{L}_{all} = \mathcal{L}_{task} + \lambda_{cd} \times \mathcal{L}_{CD} + \lambda_{sd} \times \mathcal{L}_{SD}. \quad (8)$$

Here, \mathcal{L}_{task} denotes the tracking task loss [39]. λ_{cd} and λ_{sd} are the loss coefficients corresponding to the two loss terms, respectively. In our study, we set the ratio of λ_{sd} and λ_{cd} to 2:1, respectively.

F. Implementation Details

We choose OTrack [39] as our foundational tracker, employing ViT [40] as its feature extractor. For parameter initialization, we utilize the original pre-trained model of OTrack-base-256 [39]. For each sequence in a given training set, we collect the training samples and subject them to standard data augmentation operations, including rotation, translation, and gray-scale, aligning with the data processing scheme of the base tracker [39]. During training, the entire model utilizes AdamW to minimize the classification and regression loss functions. We use the LasHeR training set to train the entire tracking network in an end-to-end manner, which is used to evaluate GTOT [43], RGBT210 [44], RGBT234 [45], and LasHeR [11]. For the evaluation of VTUAV [46], we utilize

the training set from VTUAV as the training data. In addition, we set the learning rate of the backbone network to 5e-6, and the tracking head to 5e-5. The CKD implementation is conducted on the PyTorch platform using two Nvidia A100 GPUs with 40G memory, and a global batch size of 40. The model fine-tuning takes 30 epochs that each epoch contains 60000 sample pairs. For VTUAV, we fine-tuned 5 epochs.

G. Evaluation Dataset and Protocol

1) *Dataset*: GTOT dataset is the earliest RGBT tracking dataset, consisting of 50 RGBT video sequences with a total of around 15,000 frames. However, the average sequence length of 150 frames in the dataset limits a comprehensive evaluation of model performance. RGBT210 dataset expands the scope by including 210 pairs of RGBT video sequences, amounting to approximately 209.4K frames. RGBT234 dataset is an upgrade from RGBT210 consists of 234 highly aligned RGBT video pairs, totaling approximately 233.4K frames. Importantly, it provides more accurate bounding box annotations and annotations for 12 challenge attributes. LasHeR dataset is the largest RGBT tracking dataset, containing 1224 aligned video sequences with a total number of frames up to 1469.6K frames. It provides 245 test sequences and 979 training sequences, which can comprehensively evaluate tracking performance. VTUAV dataset collects RGBT data from UAV scenarios, expanding the application of RGBT tracking. Our experiments primarily focus on the short-term tracking subset of this dataset.

2) *Protocol*: In our study, we utilize precision rate (PR) and success rate (SR) as the main evaluation metrics for one-pass evaluation (OPE), which are commonly employed in current RGBT tracking tasks. These metrics enable a quantitative analysis of tracking performance. PR evaluates the fraction of frames where the distance between the tracker’s output position and the true bounding box value falls below a predetermined threshold. Note that, we set the threshold to 5 pixels for the GTOT dataset and 20 pixels for other datasets, thereby calculating a representative PR score. SR the percentage of successfully tracked frames whose Intersection over Union (IoU) is greater than a specified threshold, and then SR metric is calculated by varying the threshold and computing the Area Under the Curve (AUC) of the resultant curve. To eliminate these effects, the PR is normalized using the scale of the ground truth box to calculate the NPR. The normalized accuracy curve can be obtained by changing the normalization threshold, and the region under the normalized accuracy curve with the normalization threshold in the range of [0, 0.5] is calculated as the representative NPR score.

H. Quantitative Comparison

We evaluate our algorithm on five popular RGBT tracking benchmarks and compare its performance with current state-of-the-art trackers. The effectiveness of our proposed method is demonstrated in Table I, which provides a summary of the comparison results.

TABLE I
PR/NPR AND SR SCORES (%) FOR ADVANCED TRACKERS ON FIVE DATASETS.. THE BEST AND SECOND ARE THE RESULT OF THE RED AND BLUE.

Methods	Pub. Info.	Backbone	GTOT		RGBT210		RGBT234		LasHeR			VTUAV		FPS ↑
			PR↑	SR↑	PR↑	SR↑	PR↑	SR↑	PR↑	NPR↑	SR↑	PR↑	SR↑	
MANet [22]	ICCVW 2019	VGG-M	89.4	72.4	-	-	77.7	53.9	45.5	38.3	32.6	-	-	1
DAPNet [47]	ACM MM 2019	VGG-M	88.2	70.7	-	-	76.6	53.7	43.1	38.3	31.4	-	-	2
mfDiMP [20]	ICCVW 2019	ResNet-50	83.6	69.7	78.6	55.5	-	-	44.7	39.5	34.3	67.3	55.4	10.3
CMPP [48]	CVPR 2020	VGG-M	92.6	73.8	-	-	82.3	57.5	-	-	-	-	-	1.3
CAT [49]	ECCV 2020	VGG-M	88.9	71.7	79.2	53.3	80.4	56.1	45.0	39.5	31.4	-	-	20
ADNet [23]	IJCV 2021	VGG-M	90.4	73.9	-	-	80.7	57.0	-	-	-	62.2	46.6	25
JMMAC [50]	TIP 2021	VGG-M	90.2	73.2	-	-	79.0	57.3	-	-	-	-	-	4
MANet++ [1]	TIP 2021	VGG-M	88.2	70.7	-	-	80.0	55.4	46.7	40.4	31.4	-	-	25.4
APFNet [14]	AAAI 2022	VGG-M	90.5	73.7	-	-	82.7	57.9	50.0	43.9	36.2	-	-	1.3
DMCNet [3]	TNNLS 2022	VGG-M	90.9	73.3	79.7	55.5	83.9	59.3	49.0	43.1	35.5	-	-	2.3
ProTrack [16]	ACM MM 2022	ViT-B	-	-	-	-	78.6	58.7	50.9	-	42.1	-	-	30
MIRNet [51]	ICME 2022	VGG-M	90.9	74.4	-	-	81.6	58.9	-	-	-	-	-	30
HMFT [46]	CVPR 2022	ResNet-50	91.2	74.9	78.6	53.5	78.8	56.8	-	-	-	75.8	62.7	30.2
MFG [52]	TMM 2022	ResNet-18	88.9	70.7	74.9	46.7	75.8	51.5	-	-	-	-	-	-
DFNet [53]	TITS 2022	VGG-M	88.1	71.9	-	-	77.2	51.3	-	-	-	-	-	-
MACFT [54]	Sensors 2023	ViT-B	-	-	-	-	85.7	62.2	65.3	-	51.4	80.1	66.8	22
CMD [4]	CVPR 2023	ResNet-50	89.2	73.4	-	-	82.4	58.4	59.0	54.6	46.4	-	-	30
ViPT [15]	CVPR 2023	ViT-B	-	-	-	-	83.5	61.7	65.1	-	52.5	-	-	-
TBSI [5]	CVPR 2023	ViT-B	-	-	85.3	62.5	87.1	63.7	69.2	65.7	55.6	-	-	36.2
QAT [12]	ACM MM 2023	ResNet-50	91.5	75.5	86.8	61.9	88.4	64.4	64.2	59.6	50.1	80.1	66.7	22
BAT [6]	AAAI 2024	ViT-B	-	-	-	-	86.8	64.1	70.2	-	56.3	-	-	-
TATrack [55]	AAAI 2024	ViT-B	-	-	85.3	61.8	87.2	64.4	70.2	-	56.1	-	-	26.1
OneTracker [25]	CVPR 2024	ViT-B	-	-	-	-	85.7	64.2	67.2	-	53.8	-	-	-
Un-Track [56]	CVPR 2024	ViT-B	-	-	-	-	84.2	62.5	66.7	-	53.6	-	-	-
SDSTrack [24]	CVPR 2024	ViT-B	-	-	-	-	84.8	62.5	66.5	-	53.1	-	-	20.9
Ours	-	ViT-B	93.2	77.2	88.4	65.2	90.0	67.4	73.2	69.3	58.1	90.2	77.8	96.4

1) *Evaluation on GTOT dataset:* The comparison results on GTOT dataset are shown in Table I. Compared to state-of-the-art trackers, our method exhibits superior performance in GTOT dataset, achieving gains over QAT [12] by 1.0% in PR. We further compare our method with CMPP [48], the best-performing tracker on the PR metric for this dataset. Although the PR of our method is 0.1% below that of CMPP [48], our CKD outperforms CMPP by 2.0% in SR. As for our low PR, we attribute this to the prevalence of small objects in the GTOT dataset, for which CMPP’s feature pyramid strategy aggregates features across all layers to enhance the feature representation capabilities. Additionally, CMPP builds a historical information pool using external storage, improving the representation of the current frame. However, these strategies significantly affect the efficiency of CMPP, making our CKD approximately 90 times faster than CMPP.

2) *Evaluation on RGBT210 dataset:* As shown in Table I, CKD exceeds almost state-of-the-art trackers in RGBT210 dataset. Compared to mfDiMP [46], which is the winner of VOT2019-RGBT, CKD achieves significant improvements in PR/SR with a gain of 9.8%/9.7%. Moreover, compared with TBSI [5], which is the second best-performing algorithms in terms of SR, CKD outperforms it by 2.9%/2.7% on the PR/SR metrics. We further compare CKD with QAT [12], which are the second best-performing algorithms in terms of PR, and CKD outperforms it by 1.6%/3.3% on PR/SR.

3) *Evaluation on RGBT234 dataset:* To further evaluate the effectiveness of CKD, we conduct a series of experiments on RGBT234 dataset, including overall and attribute-based comparison.

Overall Comparison. RGBT234 dataset is one of the most important datasets in the field of RGBT tracking, and also the dataset with the most evaluation results of existing algorithms. Therefore, we evaluate CKD against 24 state-of-the-art RGBT trackers on RGBT234 dataset. The evaluation results are presented in Table I. CKD outperforms all state-of-the-art RGBT methods in PR/SR metrics, and obtains new SOTA results of 90.0%/67.4% in PR/SR. Compared with QAT [12] and TATrack [55] algorithms, which are the second best-performing algorithms in terms of PR and SR, respectively, CKD outperforms them by 1.6% and 3.0% in both PR and SR metrics.

Challenge-based Comparison. We also present the results of CKD against the most advanced RGBT trackers available, including BAT [6], SDSTrack [24], TBSI [5], and ViPT [15], on different challenge subsets. The evaluation results are shown in 4, where the marks of each corner represent the attributes of the challenge subset and the highest and lowest performance under that attribute, respectively. These attributes include no occlusion (NO), partial occlusion (PO), heavy occlusion (HO), low illumination (LI), low resolution (LR), thermal crossover (TC), deformation (DEF), fast motion (FM),

scale variation (SV), motion blur (MB), camera moving (CM) and background clutter (BC). The results show that our method performs best in all challenge subsets, and it proves that CKD has great potential in various complex tracking scenarios.

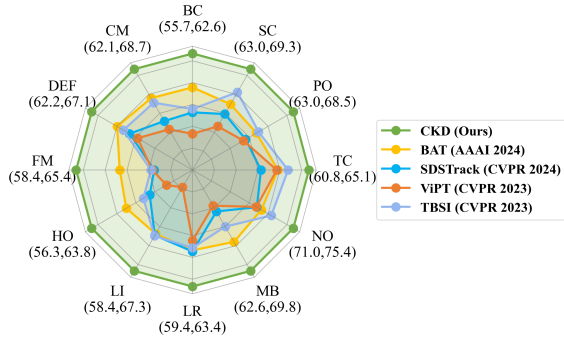


Fig. 4. Attribute-based evaluation on RGBT234 in terms of SR metric. CKD achieves the best performance on all attribute splits. Axes of each attribute have been normalized.

4) *Evaluation on LasHeR dataset:* We compare 16 state-of-the-art RGBT trackers on LasHeR dataset, which is currently the largest and most challenging RGBT tracking dataset, and the evaluation results are shown in Table I. CKD again outperforms all existing trackers by a clear margin. For instance, compared to BAT [6], the second best performing algorithm in this dataset, CKD exhibits a 3.0%/2.0% performance advantage on PR/SR metrics. The experiment further verifies the effectiveness of our approach in more complex scenarios.

5) *Evaluation on VTUAV dataset:* We evaluate the proposed method CKD on VTUAV dataset, a recently proposed drone perspective RGBT tracking dataset. From Table I, it can be seen that CKD obtains 90.2%/77.8% on PR and SR metrics, which again confirm its effectiveness. Moreover, CKD surpasses the state-of-the-art MACFT [54] by 10.1% and 11.0% in PR and SR scores, respectively. The experiment further verifies the effectiveness of our approach in drone tracking scenarios.

I. Ablation Study

To verify the effectiveness of the proposed method, several ablation studies are performed on RGBT234 and LasHeR datasets.

TABLE II
ABLATION STUDY ON THE MAIN COMPONENTS OF CKD.

	Pretrained model	RGBT234		LasHeR	
		PR	SR	PR	SR
baseline	SOT	86.4	64.5	67.8	54.0
w/ SD	SOT	86.4	65.0	68.9	54.5
w/ SD CD	SOT	87.4	65.5	71.6	56.9
w/ SD CD MM	SOT	88.6	66.1	72.3	57.4
w/ SD CD MM	DropMAE	90.4	67.8	73.1	58.0

1) *Component Analysis:* In Table II, we conduct ablation studies on RGBT234 and LasHeR datasets to verify the effectiveness of different designed modules in CKD. Our baseline

TABLE III
ABLATION STUDY ON THE DIFFERENT ELIMINATION SCHEME.

	RGBT234		LasHeR		MACs(G)	FPS
	PR	SR	PR	SR		
CKD _{slow}	90.4	67.8	73.1	58.0	57.802	84.8
w/ CE [39]	88.7	66.5	73.0	58.0	42.735	96.4
w/ MCE	90.0	67.4	73.2	58.1	42.735	96.4

structure is the same as CKD, along with consistent training data and task losses, to fairly verify the effectiveness of the proposed components.

w/ *SD* denotes the baseline equipped with style distillation, which achieves a certain improvement. The experiment shows that aligning modality styles is effective, but there are limitations.

w/ *SD CD* indicates that adding content distillation to w/ *SD* results in significant performance improvements. The experiment shows that it is crucial to preserve the stability of modality content representation, as unconstrained style distillation could harm modality content representation, which could explain the limitations of w/ *SD*.

w/ *SD CD MM* represents that adding masked modeling to w/ *SD CD*. The experiment demonstrates the effectiveness of the masked modeling strategy.

2) *Impact of Pretrained model:* We also explore the DropMAE [57] pretrained model trained on the Kinetics700 dataset [58] as our pretrained model, which further achieves significant performance gains. Compared to the "SOT" pretrained model usually exploited by existing RGBT tracking methods [5], [6], [25], [56], DropMAE can bring superior performance to RGBT tracking. The experiment provides insights to further improve RGBT performance.

3) *Effectiveness of token elimination strategy:* To verify the effectiveness of the proposed multi-modal candidate token elimination strategy, we evaluate different token elimination methods in Table III. Here, CKD_{slow} represents the CKD method without a token elimination strategy, but it is still faster than existing RGBT trackers.

w/ *CE* [39] indicates that the two student branches individually apply the candidate token elimination strategy, following [39]. However, although CE brings an improvement in tracking efficiency, it also causes a significant performance drop.

w/ *MCE* indicates that the two student branches follow the proposed multi-modal candidate token elimination strategy for collaborative token elimination. It can be seen that MCE achieves a balance between tracking efficiency and accuracy.

4) *Hyper-parameter sensitivity analysis:* We analyze the parameter sensitivity as follows.

Impact of loss weights. We explore the influence of different loss weights between style and distillation losses on CKD performance in Figure 5. From Figure 5 it can be observed that the two kinds of losses in CKD are robust to the hyperparameters for these weights.

Impact of masked ratios. As shown in Table IV, we analyze the influence of different masked ratios on masked modeling strategy in CKD. It can be observed that the performance

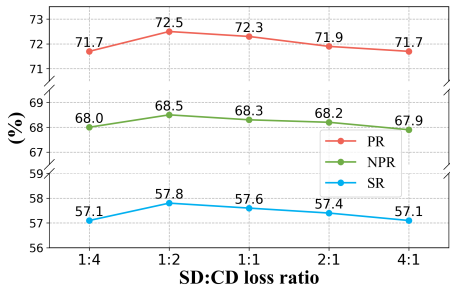


Fig. 5. Ablation study of loss weights on LasHeR dataset.

TABLE IV
ABLATION STUDY ON DIFFERENT MASKED RATIOS.

	RGBT234		LasHeR		
	PR	SR	PR	NPR	SR
CKD w/ mask 0%	87.4	65.5	71.6	67.5	56.9
CKD w/ mask 25%	88.6	66.1	72.3	68.1	57.4
CKD w/ mask 50%	88.2	65.1	71.4	67.2	56.9
CKD w/ mask 75%	88.2	64.3	70.6	66.7	56.4

of CKD is always improved after the introduction of mask modeling, but the performance decreases slightly with the increase of mask modeling.

5) *Analysis of feature decoupling scheme:* In Table V, we design several variants to verify the effectiveness of feature decoupling.

baseline w/ IN denotes the introduction of instance normalization in both student branches, which performs tracking with only content features. The experiment shows that modality style features certain discriminative information, which can lead to performance loss when directly dropped.

baseline w/ FD represents the introduction of non-decoupled feature distillation (FD) only between two student branches. The experiment suggests that the non-decoupled distillation scheme may harm the modality content representation.

baseline w/ SD is to perform distillation only in the style features between two student branches. The experiment further verifies that performing distillation for all modal features is unnecessary.

baseline w/ CKD is the coupled distillation scheme proposed in this paper. The experiment further demonstrating that the importance of feature decoupling scheme.

6) *Visual analysis:* In Figure 6, we visualize and compare the TIR content features extracted by the models trained with different distillation methods and not trained with distilla-

TABLE V
ABLATION STUDY ON THE FEATURE DECOUPLING SCHEME.

	RGBT234		LasHeR		
	PR	SR	PR	NPR	SR
baseline	86.4	64.5	67.8	64.3	54.0
baseline w/ IN	85.6	63.7	67.1	63.2	53.4
baseline w/ FD	85.2	63.8	67.2	63.4	53.7
baseline w/ SD	86.4	65.0	68.9	64.3	54.5
baseline w/ CKD	87.4	65.5	71.6	67.5	56.9

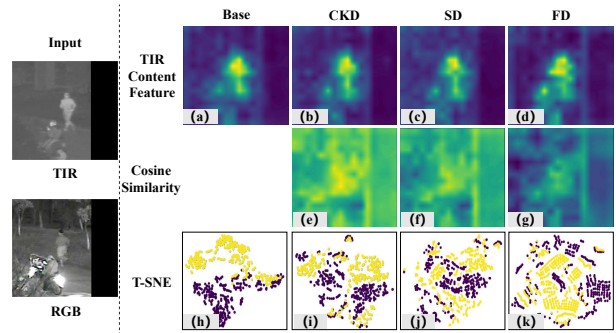


Fig. 6. Comparison of feature maps and T-SNE visualizations for different distillation methods. For T-SNE maps, they have the same scale of axes. The hotter color in the first row indicates more salient features, while in the second row the hotter color indicates more similar between the non-distilled (Base features) and distilled features, and vice versa. In the third row, the yellow and purple color indicate the features of RGB and TIR modalities respectively.

tion methods, and show their similarity relationships. The experiment shows that the proposed CKD method achieves a good balance between modality gap elimination and modality content representation preservation.

IV. CONCLUSION

In this work, we present a novel Coupled Knowledge Distillation (CKD) for RGBT tracking, which is the first effort to break the modality gap challenge in RGBT tracking. We first analyze the influence of modality style on modality gap, and then the proposed CKD can effectively enhance the consistency of modality style and avoid harming to modality content representation. Moreover, the proposed masked modeling strategy and a multi-modal candidate token elimination strategy effectively improve tracking performance and efficiency. Extensive experiments demonstrate the superiority of the proposed method. In the future, we will explore the benefits of the proposed CKD in other multi-modal visual tasks, such as RGBD/RGBE tracking [59], [60], image fusion [61], [62] and collaborative learning [63].

REFERENCES

- [1] A. Lu, C. Li, Y. Yan, J. Tang, and B. Luo, "Rgbt tracking via multi-adapter network with hierarchical divergence loss," *IEEE Transactions on Image Processing*, vol. 30, pp. 5613–5625, 2021.
- [2] Z. Cui, L. Zhou, C. Wang, C. Xu, and J. Yang, "Visual micro-pattern propagation," *IEEE Transactions on Pattern Analysis and Machine Intelligence*, vol. 45, no. 1, pp. 1267–1286, 2022.
- [3] A. Lu, C. Qian, C. Li, J. Tang, and L. Wang, "Duality-gated mutual condition network for rgbt tracking," *IEEE Transactions on Neural Networks and Learning Systems*, 2022.
- [4] T. Zhang, H. Guo, Q. Jiao, Q. Zhang, and J. Han, "Efficient rgb-t tracking via cross-modality distillation," in *Proceedings of the IEEE/CVF Conference on Computer Vision and Pattern Recognition*, 2023, pp. 5404–5413.
- [5] T. Hui, Z. Xun, F. Peng, J. Huang, X. Wei, X. Wei, J. Dai, J. Han, and S. Liu, "Bridging search region interaction with template for rgb-t tracking," in *Proceedings of the IEEE/CVF Conference on Computer Vision and Pattern Recognition*, 2023, pp. 13 630–13 639.
- [6] B. Cao, J. Guo, P. Zhu, and Q. Hu, "Bi-directional adapter for multi-modal tracking," in *Proceedings of the AAAI Conference on Artificial Intelligence*, 2024.
- [7] A. Zheng, J. Liu, Z. Wang, L. Huang, C. Li, and B. Yin, "Visible-infrared person re-identification via specific and shared representations learning," *Visual Intelligence*, vol. 1, no. 1, p. 29, 2023.

- [8] A. Zheng, Z. Wang, Z. Chen, C. Li, and J. Tang, "Robust multi-modality person re-identification," in *Proceedings of the AAAI Conference on Artificial Intelligence*, 2021, pp. 3529–3537.
- [9] Z. Wang, C. Li, A. Zheng, R. He, and J. Tang, "Interact, embed, and enlarge: Boosting modality-specific representations for multi-modal person re-identification," in *Proceedings of the AAAI Conference on Artificial Intelligence*, 2022, pp. 2633–2641.
- [10] K. Wang, Z. Tu, C. Li, C. Zhang, and B. Luo, "Learning adaptive fusion bank for multi-modal salient object detection," *IEEE Transactions on Circuits and Systems for Video Technology*, 2024.
- [11] C. Li, W. Xue, Y. Jia, Z. Qu, B. Luo, J. Tang, and D. Sun, "Lasher: A large-scale high-diversity benchmark for rgbt tracking," *IEEE Transactions on Image Processing*, vol. 31, pp. 392–404, 2021.
- [12] L. Liu, C. Li, Y. Xiao, and J. Tang, "Quality-aware rgbt tracking via supervised reliability learning and weighted residual guidance," in *Proceedings of the 31st ACM International Conference on Multimedia*, 2023, pp. 3129–3137.
- [13] Z. Cheng, A. Lu, Z. Zhang, C. Li, and L. Wang, "Fusion tree network for rgbt tracking," in *IEEE International Conference on Advanced Video and Signal Based Surveillance*, 2022, pp. 1–8.
- [14] Y. Xiao, M. Yang, C. Li, L. Liu, and J. Tang, "Attribute-based progressive fusion network for rgbt tracking," in *Proceedings of the AAAI Conference on Artificial Intelligence*, 2022, pp. 2831–2838.
- [15] J. Zhu, S. Lai, X. Chen, D. Wang, and H. Lu, "Visual prompt multi-modal tracking," in *Proceedings of the IEEE/CVF Conference on Computer Vision and Pattern Recognition*, 2023, pp. 9516–9526.
- [16] J. Yang, Z. Li, F. Zheng, A. Leonardis, and J. Song, "Prompting for multi-modal tracking," in *Proceedings of the 30th ACM International Conference on Multimedia*, 2022, pp. 3492–3500.
- [17] L. Huang, J. Qin, Y. Zhou, F. Zhu, L. Liu, and L. Shao, "Normalization techniques in training dnns: Methodology, analysis and application," *IEEE Transactions on Pattern Analysis and Machine Intelligence*, 2023.
- [18] X. Huang and S. Belongie, "Arbitrary style transfer in real-time with adaptive instance normalization," in *Proceedings of the IEEE international conference on computer vision*, 2017, pp. 1501–1510.
- [19] Y. Zhu, C. Li, J. Tang, and B. Luo, "Quality-aware feature aggregation network for robust rgbt tracking," *IEEE Transactions on Intelligent Vehicles*, 2020.
- [20] L. Zhang, M. Danelljan, A. Gonzalez-Garcia, J. van de Weijer, and F. Shahbaz Khan, "Multi-modal fusion for end-to-end rgb-t tracking," in *Proceedings of the IEEE International Conference on Computer Vision Workshops*, 2019.
- [21] Z. Tang, T. Xu, H. Li, X.-J. Wu, X. Zhu, and J. Kittler, "Exploring fusion strategies for accurate rgbt visual object tracking," *Information Fusion*, p. 101881, 2023.
- [22] C. Li, A. Lu, A. Zheng, Z. Tu, and J. Tang, "Multi-adapter rgbt tracking," in *Proceedings of IEEE International Conference on Computer Vision Workshops*, 2019.
- [23] P. Zhang, D. Wang, H. Lu, and X. Yang, "Learning adaptive attribute-driven representation for real-time rgb-t tracking," *International Journal of Computer Vision*, vol. 129, pp. 2714–2729, 2021.
- [24] X. Hou, J. Xing, Y. Qian, Y. Guo, S. Xin, J. Chen, K. Tang, M. Wang, Z. Jiang, L. Liu *et al.*, "Sdstrack: Self-distillation symmetric adapter learning for multi-modal visual object tracking," in *Proceedings of IEEE Conference on Computer Vision and Pattern Recognition*, 2024.
- [25] L. Hong, S. Yan, R. Zhang, W. Li, X. Zhou, P. Guo, K. Jiang, Y. Chen, J. Li, Z. Chen *et al.*, "Onetracker: Unifying visual object tracking with foundation models and efficient tuning," in *Proceedings of IEEE Conference on Computer Vision and Pattern Recognition*, 2024.
- [26] G. Hinton, O. Vinyals, and J. Dean, "Distilling the knowledge in a neural network," *arXiv preprint arXiv:1503.02531*, 2015.
- [27] K. Song, J. Xie, S. Zhang, and Z. Luo, "Multi-mode online knowledge distillation for self-supervised visual representation learning," in *Proceedings of the IEEE/CVF Conference on Computer Vision and Pattern Recognition*, 2023, pp. 11 848–11 857.
- [28] D. Chen, J.-P. Mei, Y. Zhang, C. Wang, Z. Wang, Y. Feng, and C. Chen, "Cross-layer distillation with semantic calibration," in *Proceedings of the AAAI Conference on Artificial Intelligence*, 2021, pp. 7028–7036.
- [29] J. Yuan, M. H. Phan, L. Liu, and Y. Liu, "Fakd: Feature augmented knowledge distillation for semantic segmentation," in *Proceedings of the IEEE/CVF Winter Conference on Applications of Computer Vision*, 2024, pp. 595–605.
- [30] G. Guo, L. Han, L. Wang, D. Zhang, and J. Han, "Semantic-aware knowledge distillation with parameter-free feature uniformization," *Visual Intelligence*, vol. 1, no. 1, p. 6, 2023.
- [31] J. Zhu, S. Tang, D. Chen, S. Yu, Y. Liu, M. Rong, A. Yang, and X. Wang, "Complementary relation contrastive distillation," in *Proceedings of the IEEE/CVF conference on computer vision and pattern recognition*, 2021, pp. 9260–9269.
- [32] Q. Qian, H. Li, and J. Hu, "Improved knowledge distillation via full kernel matrix transfer," in *Proceedings of the 2022 SIAM International Conference on Data Mining (SDM)*. SIAM, 2022, pp. 612–620.
- [33] J. Shen, Y. Liu, X. Dong, X. Lu, F. S. Khan, and S. Hoi, "Distilled siamese networks for visual tracking," *IEEE Transactions on Pattern Analysis and Machine Intelligence*, vol. 44, no. 12, pp. 8896–8909, 2021.
- [34] P. Sarkar and A. Etemad, "Xkd: Cross-modal knowledge distillation with domain alignment for video representation learning," in *Proceedings of the AAAI Conference on Artificial Intelligence*, vol. 38, no. 13, 2024, pp. 14 875–14 885.
- [35] S. Ren, Y. Du, J. Lv, G. Han, and S. He, "Learning from the master: Distilling cross-modal advanced knowledge for lip reading," in *Proceedings of the IEEE/CVF Conference on Computer Vision and Pattern Recognition*, 2021, pp. 13 325–13 333.
- [36] L. Zhao, X. Peng, Y. Chen, M. Kapadia, and D. N. Metaxas, "Knowledge as priors: Cross-modal knowledge generalization for datasets without superior knowledge," in *Proceedings of the IEEE/CVF Conference on Computer Vision and Pattern Recognition*, 2020, pp. 6528–6537.
- [37] R. Dai, S. Das, and F. Bremond, "Learning an augmented rgb representation with cross-modal knowledge distillation for action detection," in *Proceedings of the IEEE/CVF International Conference on Computer Vision*, 2021, pp. 13 053–13 064.
- [38] P. Lee, T. Kim, M. Shim, D. Wee, and H. Byun, "Decomposed cross-modal distillation for rgb-based temporal action detection," in *Proceedings of the IEEE/CVF Conference on Computer Vision and Pattern Recognition*, 2023, pp. 2373–2383.
- [39] B. Ye, H. Chang, B. Ma, S. Shan, and X. Chen, "Joint feature learning and relation modeling for tracking: A one-stream framework," in *European Conference on Computer Vision*. Springer, 2022, pp. 341–357.
- [40] A. Dosovitskiy, L. Beyer, A. Kolesnikov, D. Weissenborn, X. Zhai, T. Unterthiner, M. Dehghani, M. Minderer, G. Heigold, S. Gelly *et al.*, "An image is worth 16x16 words: Transformers for image recognition at scale," *arXiv preprint arXiv:2010.11929*, 2020.
- [41] K. He, X. Chen, S. Xie, Y. Li, P. Dollár, and R. Girshick, "Masked autoencoders are scalable vision learners," in *Proceedings of the IEEE/CVF conference on computer vision and pattern recognition*, 2022, pp. 16 000–16 009.
- [42] Y. Chen, Y. Liu, D. Jiang, X. Zhang, W. Dai, H. Xiong, and Q. Tian, "Sdae: Self-distilled masked autoencoder," in *European conference on computer vision*, 2022, pp. 108–124.
- [43] C. Li, H. Cheng, S. Hu, X. Liu, J. Tang, and L. Lin, "Learning collaborative sparse representation for grayscale-thermal tracking," *IEEE Trans. Image Process.*, vol. 25, no. 12, pp. 5743–5756, 2016.
- [44] C. Li, N. Zhao, Y. Lu, C. Zhu, and J. Tang, "Weighted sparse representation regularized graph learning for rgb-t object tracking," in *Proceedings of ACM International Conference on Multimedia*, 2017.
- [45] C. Li, X. Liang, Y. Lu, N. Zhao, and J. Tang, "Rgb-t object tracking: benchmark and baseline," *Pattern Recognition*, vol. 96, p. 106977, 2019.
- [46] Z. Pengyu, J. Zhao, D. Wang, H. Lu, and X. Ruan, "Visible-thermal uav tracking: A large-scale benchmark and new baseline," in *Proceedings of the IEEE conference on computer vision and pattern recognition*, 2022.
- [47] Y. Zhu, C. Li, B. Luo, J. Tang, and X. Wang, "Dense feature aggregation and pruning for rgbt tracking," in *Proceedings of ACM International Conference on Multimedia*, 2019.
- [48] C. Wang, C. Xu, Z. Cui, L. Zhou, and J. Yang, "Cross-modal pattern-propagation for rgb-t tracking," in *Proceedings of the IEEE Conference on Computer Vision and Pattern Recognition*, 2020.
- [49] C. Li, L. Liu, A. Lu, Q. Ji, and J. Tang, "Challenge-aware rgbt tracking," in *Proceedings of the IEEE European Conference on Computer Vision*, 2020.
- [50] P. Zhang, J. Zhao, D. Wang, H. Lu, and X. Yang, "Jointly modeling motion and appearance cues for robust rgb-t tracking," *IEEE Transactions on Image Processing*, 2020.
- [51] R. Hou, T. Ren, and G. Wu, "Mirmet: A robust rgbt tracking jointly with multi-modal interaction and refinement," in *2022 IEEE International Conference on Multimedia and Expo (ICME)*, 2022, pp. 1–6.

- [52] X. Wang, X. Shu, S. Zhang, B. Jiang, Y. Wang, Y. Tian, and F. Wu, "Mfgnet: Dynamic modality-aware filter generation for rgb-t tracking," *IEEE Transactions on Multimedia*, 2022.
- [53] J. Peng, H. Zhao, and Z. Hu, "Dynamic fusion network for rgbt tracking," *IEEE Transactions on Intelligent Transportation Systems*, vol. 24, no. 4, pp. 3822–3832, 2022.
- [54] Y. Luo, X. Guo, M. Dong, and J. Yu, "Learning modality complementary features with mixed attention mechanism for rgb-t tracking," *Sensors*, vol. 23, no. 14, p. 6609, 2023.
- [55] H. Wang, X. Liu, Y. Li, M. Sun, D. Yuan, and J. Liu, "Temporal adaptive rgbt tracking with modality prompt," in *Proceedings of the AAAI Conference on Artificial Intelligence*, 2024.
- [56] Z. Wu, J. Zheng, X. Ren, F.-A. Vasluianu, C. Ma, D. P. Paudel, L. Van Gool, and R. Timofte, "Single-model and any-modality for video object tracking," in *Proceedings of IEEE Conference on Computer Vision and Pattern Recognition*, 2024.
- [57] Q. Wu, T. Yang, Z. Liu, B. Wu, Y. Shan, and A. B. Chan, "Dropmae: Masked autoencoders with spatial-attention dropout for tracking tasks," in *Proceedings of the IEEE/CVF Conference on Computer Vision and Pattern Recognition*, 2023, pp. 14 561–14 571.
- [58] J. Carreira, E. Noland, C. Hillier, and A. Zisserman, "A short note on the kinetics-700 human action dataset," *arXiv preprint arXiv:1907.06987*, 2019.
- [59] X.-F. Zhu, T. Xu, Z. Tang, Z. Wu, H. Liu, X. Yang, X.-J. Wu, and J. Kittler, "Rgbd1k: A large-scale dataset and benchmark for rgb-d object tracking," in *Proceedings of the AAAI Conference on Artificial Intelligence*, vol. 37, no. 3, 2023, pp. 3870–3878.
- [60] Z. Zhu, J. Hou, and D. O. Wu, "Cross-modal orthogonal high-rank augmentation for rgb-event transformer-trackers," in *Proceedings of the IEEE/CVF International Conference on Computer Vision*, 2023, pp. 22 045–22 055.
- [61] W. Zhao, S. Xie, F. Zhao, Y. He, and H. Lu, "Metafusion: Infrared and visible image fusion via meta-feature embedding from object detection," in *Proceedings of the IEEE/CVF Conference on Computer Vision and Pattern Recognition*, 2023, pp. 13 955–13 965.
- [62] J. Liu, Z. Liu, G. Wu, L. Ma, R. Liu, W. Zhong, Z. Luo, and X. Fan, "Multi-interactive feature learning and a full-time multi-modality benchmark for image fusion and segmentation," in *Proceedings of the IEEE/CVF international conference on computer vision*, 2023, pp. 8115–8124.
- [63] P. Xu, X. Zhu, and D. A. Clifton, "Multimodal learning with transformers: A survey," *IEEE Transactions on Pattern Analysis and Machine Intelligence*, 2023.